Neuron, Vol. 23, 297–308, June, 1999, Copyright ©1999 by Cell Press

Leukocyte Infiltration, Neuronal Degeneration, and Neurite Outgrowth after Ablation of Scar-Forming, Reactive Astrocytes in Adult Transgenic Mice

Toby G. Bush,*†‖ Narman Puvanachandra,*† Catherine H. Horner,*† Anabella Polito,*† Thor Ostenfeld,* Clive N. Svendsen,* Lennart Mucke,‡ Martin H. Johnson,† and Michael V. Sofroniew*†§

*Medical Research Council
Cambridge Centre for Brain Repair
†Department of Anatomy
University of Cambridge
Forvie Site, Robinson Way
Cambridge CB2 2PY
United Kingdom
‡The Gladstone Molecular Neurobiology Program
and Department of Neurology
University of California, San Francisco
San Francisco, California 94141

Summary

Reactive astrocytes adjacent to a forebrain stab injury were selectively ablated in adult mice expressing HSV-TK from the *Gfap* promoter by treatment with ganciclovir. Injured tissue that was depleted of GFAP-positive astrocytes exhibited (1) a prolonged 25-fold increase in infiltration of CD45-positive leukocytes, including ultrastructurally identified monocytes, macrophages, neutrophils, and lymphocytes, (2) failure of blood–brain barrier (BBB) repair, (3) substantial neuronal degeneration that could be attenuated by chronic glutamate receptor blockade, and (4) a pronounced increase in local neurite outgrowth. These findings show that genetic targeting can be used to ablate scar-forming astrocytes and demonstrate roles for astrocytes in regulating leukocyte trafficking, repairing the BBB, protecting neurons, and restricting nerve fiber growth after injury in the adult central nervous system.

Introduction

Injury, infection, and degenerative disease in the central nervous systems (CNS) are invariably accompanied by the hypertrophy, altered gene expression, and proliferation of astrocytes, a process commonly referred to as reactive astrocytosis. While much is known about molecules that either influence, or are produced by, reactive astrocytes (Eddleston and Mucke, 1993; Ridet et al., 1997), the functions of these cells are incompletely understood. Considerable evidence suggests that in uninjured CNS tissue, nonreactive astrocytes are normally involved in maintenance of the extracellular ionic environment and pH, uptake of extracellular glutamate, provision of metabolic substrates for neurons, and interactions with endothelia to create and maintain the blood–brain barrier (BBB) (Kettenmann and Ransom, 1995). The degree to which these functions are sustained, augmented, or lost by astrocytes that become reactive after tissue injury is uncertain. In addition, it has long been hypothesized that scar-forming reactive astrocytes represent a major obstacle to axon regeneration in the injured mammalian CNS (Ramon y Cajal, 1928), but a direct test of this hypothesis by ablation of these cells or molecules that they produce in vivo has not been reported.

To investigate the roles of reactive astrocytes, we targeted their cell death genetically using the promoter of the gene for glial fibrillary acidic protein (GFAP), an intermediate filament protein whose expression in the CNS is restricted to astrocytes and related cells. Although many astrocytes in the mature, uninjured CNS do not express levels of GFAP detectable with standard immunohistochemical procedures, GFAP expression is upregulated to a readily detectable level in most, if not all, reactive astrocytes after CNS injury (Eddleston and Mucke, 1993; Ridet et al., 1997). To achieve cellular ablation, we used the thymidine kinase gene of herpes simplex virus (HSV-*Tk*). Proliferating cells that express transgene-derived HSV-TK metabolize the antiviral agent ganciclovir (GCV) to toxic nucleotide analogs that disturb nucleic acid synthesis and induce cell death (Cheng et al., 1983; Borrelli et al., 1989; Heyman et al., 1989). In this manner, cell ablation can be regulated by where and when GCV is administered. We have described previously the generation of transgenic mice expressing HSV-*Tk* from the mouse *Gfap* promoter and shown that reactive, transgene-expressing astrocytes adjacent to a forebrain stab injury are ablated by GCV (Bush et al., 1998). Here, we report the effects of ablation of reactive astrocytes after forebrain stab injury through cerebral cortex, hippocampus, and thalamus in adult mice. We find that astrocytes play fundamental roles in regulating leukocyte infiltration, repairing the blood–brain barrier (BBB), protecting neurons, and restricting nerve fiber growth after CNS injury.

Results

Regulation of HSV-TK and GFAP in Astrocytes after Stab Injury

Transgene-derived HSV-TK expressed in brains of mice used in this study migrates similarly to native HSV-TK in Western blot and is localized specifically to astrocytes by immunohistochemistry (Bush et al., 1998). To compare the regulation of transgene-derived HSV-TK with that of endogenous GFAP at the single cell level, we quantitatively analyzed sections immunohistochemically double-stained for both proteins. In hippocampus, an area showing readily detectable levels of basal GFAP expression in uninjured mice, 85% of GFAP-positive cells were also positive for HSV-TK (Figures 1A–1C). After stab injury, the absolute number of GFAP- and

§To whom correspondence should be addressed (e-mail: mvs10@cam.ac.uk).
‖Present address: Department of Physiology, University of Nevada, School of Medicine, Reno, Nevada 89557.

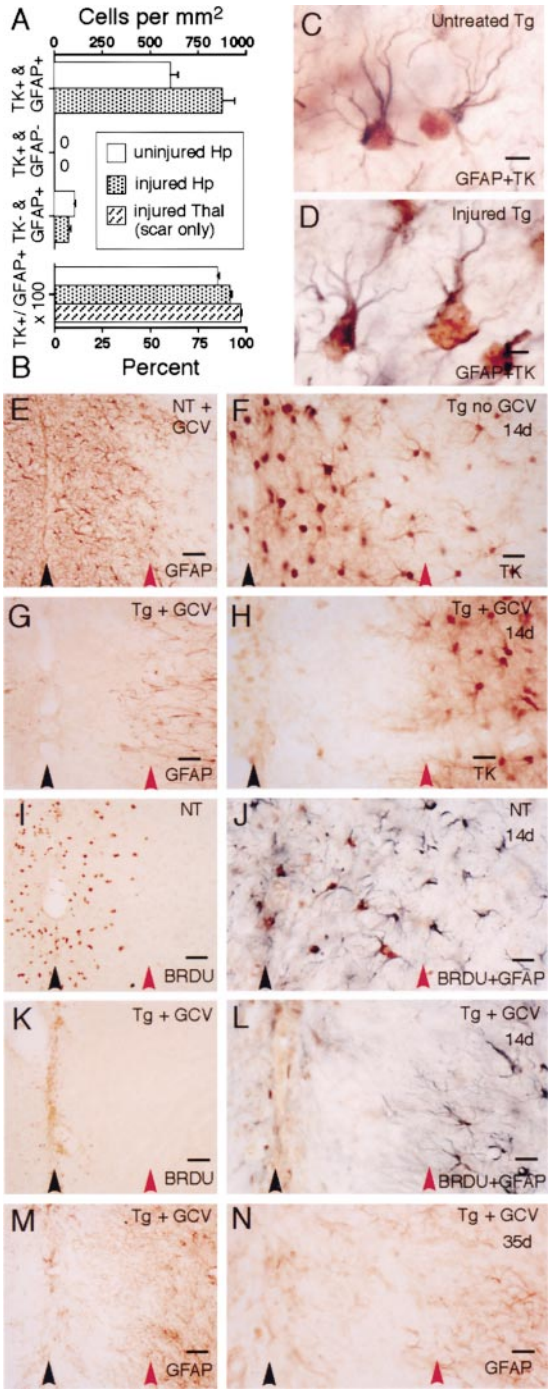

Figure 1. Cellular Expression Profile of the GFAP-HSV-TK Transgene and Selective Ablation by GCV of Proliferating, Transgene-Expressing Reactive Astrocytes

(A) Mean cell number ± SEM (n = 4 per group) of double- or single-labeled astrocytes after two-color immunohistochemistry.

(B) Percentage of double-labeled astrocytes as compared with the total number of GFAP-positive astrocytes after two-color immunohistochemistry.

(C and D) Two-color immunohistochemistry of hippocampal astrocytes in transgenic mice, untreated (C), or after stab injury (D) shows that brown-stained (HSV-TK) cell bodies and blue-stained (GFAP) processes belong to the same cells. Scale bars, 5 μm.

(E–N) One- or two-color immunohistochemistry of reactive astrocytes adjacent to stab injury (black arrowheads) in thalamus after 14 (E–L) or 35 (M and N) day survival. Single staining for GFAP (E, G, M, and N), HSV-TK (F and H), or BRDU (I and K). Double staining for BRDU (brown) and GFAP (blue) (J and L). Black and red arrowheads demarcate the zone of proliferating, scar-forming reactive astrocytes normally adjacent to stab injury, from which astrocytes have been ablated in GCV-treated transgenic mice. Scale bars: (E, G, I, K, and M), 50 μm; (F, H, J, L, and N), 20 μm.

(E) Nontransgenic (NT). GCV had no effect on astrocyte scar formation.

(F) Transgenic (Tg) not given GCV. Reactive astrocytes express HSV-TK.

(G and H) Transgenic. GCV has depleted astrocytes from wound margins. Neighboring astrocytes have upregulated GFAP or HSV-TK.

(I and J) Nontransgenic. Many BRDU- and GFAP-positive, proliferating astrocytes are present immediately adjacent to wound margins.

(K and L) Transgenic. GCV has depleted BRDU-labeled, proliferating astrocytes from wound margins. A few GFAP-negative and BRDU-positive presumptive leukocytes remain.

(M and N) Transgenic given GCV. GFAP-positive astrocytes remain depleted from wound margins after 35 days.

HSV-TK-positive cells increased, and the proportion of double-labeled cells rose to 92% (Figures 1A, 1B, and 1D). In thalamus, few cells immunoreactive for either protein could be detected in uninjured mice, whereas after injury, intensely stained GFAP- and HSV-TK-positive cells formed a densely packed scar in which the proportion of double-labeled cells was over 98%. Qualitative analysis of cerebral neocortex yielded similar observations. In all regions, some GFAP-positive cells failed to show detectable levels of HSV-TK, but this percentage was small after injury. More importantly, HSV-TK was always colocalized with GFAP, and no cells were observed in any brain region that were positive for HSV-TK but not GFAP (Figures 1A, 1C, and 1D). These findings indicate that transgene-derived HSV-TK is regulated similarly to endogenous GFAP and that nearly all reactive astrocytes, but not other cell types, express HSV-TK after CNS injury.

Effects of 7 Days of Subcutaneous GCV on Reactive Astrocytes after Stab Injury

We found previously that exposure to GCV for several days was needed to achieve substantial death of astrocytes expressing HSV-TK in vitro and that both 7 and 14 days of continuous subcutaneous (s.c.) GCV delivery were effective in ablating astrocytes immediately adjacent to forebrain stab injury (Bush et al., 1998). However, 14 days of GCV was invariably lethal to transgenic mice due to ablation of GFAP-expressing enteric glia and consequent inflammation and necrosis of the small intestine. Because 7 days of s.c. GCV was well tolerated by all mice and caused no obvious pathological changes in the bowel (Bush et al., 1998), this delivery regimen was used in the present study.

The efficiency and longevity of ablation of transgene-expressing reactive astrocytes after 7 days of s.c. GCV treatment was examined by immunohistochemical detection of GFAP and HSV-TK at 7, 14, 21, and 35 days after stab injury. Findings were indistinguishable in three groups of control mice consisting of transgenic and nontransgenic mice not given GCV, and nontransgenic mice

given GCV s.c. after injury. In these mice at 7 or 14 days after injury, there was a marked increase in the number and size of immunoreactive astrocytes along wound margins, with formation of a compact glial scar (Figures 1E and 1F). The appearance was similar at 21 days, whereas reactive astrocytosis had begun to subside by 35 days. In contrast, in GCV-treated transgenic mice at 7 or 14 days after injury, there was a pronounced reduction in the number of GFAP and HSV-TK immunoreactive astrocytes immediately adjacent to the wound that was particularly striking in thalamus, where immediate wound margins were essentially devoid of immunoreactive astrocytes for several hundred micrometers away from the center of the wound (Figures 1G and 1H). The pattern of immunohistochemical staining suggested that the death of astrocytes immediately next to the wound triggered astrocytosis in the outwardly adjacent cells after GCV delivery had stopped (Figures 1G and 1H). In addition, astrocytes were regularly ablated for much greater distances of up to several millimeters away from the stab wound in hippocampus, creating a zone essentially devoid of immunoreactive astrocytes along much of the CA1 pyramidal layer (Figures 2C and 2D). The appearance did not differ substantially at 21 days, and even at 35 days, tissue ablated of GFAP- or HSV-TK-positive cells persisted along wound margins or in CA1, in spite of varying degrees of tissue collapse (Figures 1M, 1N, and 2E), indicating that ablated astrocytes were not replaced by migrating adjacent astrocytes or precursor cells.

The effect of GCV treatment on proliferating astrocytes was examined in mice injected with BRDU on day 3 after injury, the time of peak astrocyte cell division (Amat et al., 1996). At 14 days after injury, nontransgenic animals with or without s.c. GCV treatment exhibited many BRDU-labeled cells in a narrow zone extending several hundred micrometers adjacent to the stab wound; most of these cells were identified as GFAP-positive astrocytes by double-labeling immunohistochemistry (Figures 1I and 1J). Many BRDU-labeled astrocytes were also present along the hippocampal CA1 pyramidal layer for up to several millimeters away from the wound (Figures 2A and 2F). GCV-treatment of transgenic mice ablated most BRDU-positive cells, and essentially all BRDU-labeled GFAP-positive astrocytes, including those in CA1 (Figures 1K, 1L, 2B, and 2G). Only a small number of BRDU-positive and GFAP-negative cells likely to be proliferating inflammatory cells remained. These findings demonstrate the presence of dividing GFAP-positive astrocytes in all regions where astrocyte ablation occurred and show that GCV treatment in transgenic mice killed most, if not all, dividing astrocytes.

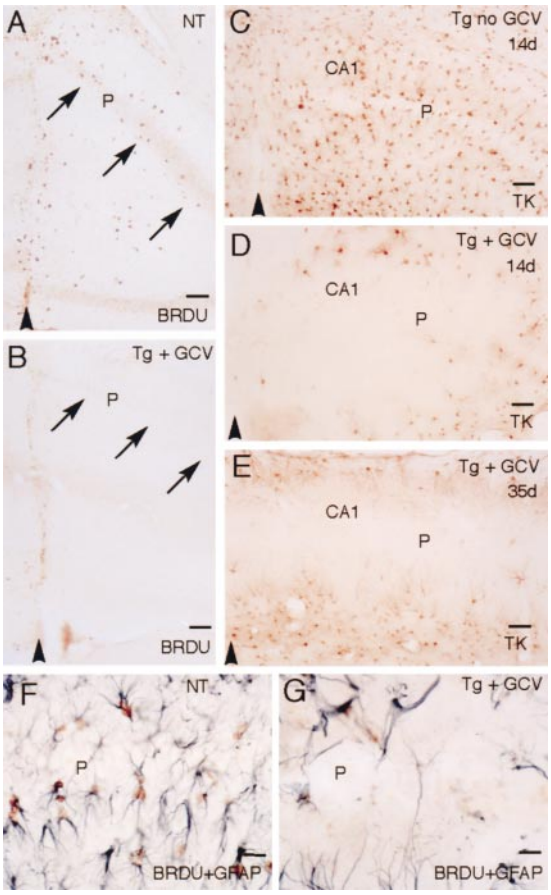

Figure 2. Proliferation, and Ablation by GCV, of Transgene-Expressing Reactive Astrocytes in Hippocampal CA1

(A–G) One- or two-color immunohistochemistry of reactive astrocytes adjacent to stab injury (arrowheads) in hippocampus after 14 (A–D, F, and G) or 35 (E) day survival. Single staining for BRDU (A and B) or HSV-TK (C–E). Double staining for BRDU (brown) and GFAP (blue) (F and G). Scale bars: (A and B), 75 μm; (C–E), 50 μm; (F and G), 20 μm.

(A and F) Nontransgenic. Many BRDU- and GFAP-positive, proliferating astrocytes are present not only immediately adjacent to wound margins, but also extending for long distances along CA1 pyramidal layer ([P], arrows).

(B and G) Transgenic. GCV has depleted BRDU-labeled, proliferating astrocytes from the wound margins as well as from the CA1 pyramidal layer ([P], arrows). Nondividing, BRDU-negative, GFAP-positive astrocytes remain.

(C) Transgenic not given GCV. Reactive astrocytes express high levels of HSV-TK in injured hippocampus.

(D and E) Transgenic. GCV has depleted proliferating astrocytes from the CA1 pyramidal layer at 14 days (D), and these have not been replaced at 35 days (E) resulting in tissue collapse. Many nondividing astrocytes adjacent to the pyramidal layer were not ablated by GCV.

Effects of Astrocyte Ablation on Tissue Integrity and Inflammatory Cells

The appearance of tissue after stab injury was indistinguishable in the three groups of control mice: transgenic and nontransgenic mice not given GCV and nontransgenic mice given GCV. The center of the stab wound was regularly defined by a narrow column of inflammatory cells (no more than several cells wide) and delimited by a thin layer of fibronectin-positive meningeal cells (Figures 3A, 3B, and 4A). Within the 400 μm of neural parenchyma immediately adjacent to the wound margin that contained scar-forming, reactive GFAP-positive astrocytes: (1) there was no evidence of interstitial edema or substantial neuronal loss in semi- or ultrathin sections; (2) activated microglia, identified as finely branched cells positive for tomato–lectin binding and light CD45 staining, were present at 7 and 14 days but had resolved in most cases by 21 or 35 days; (3) intensely

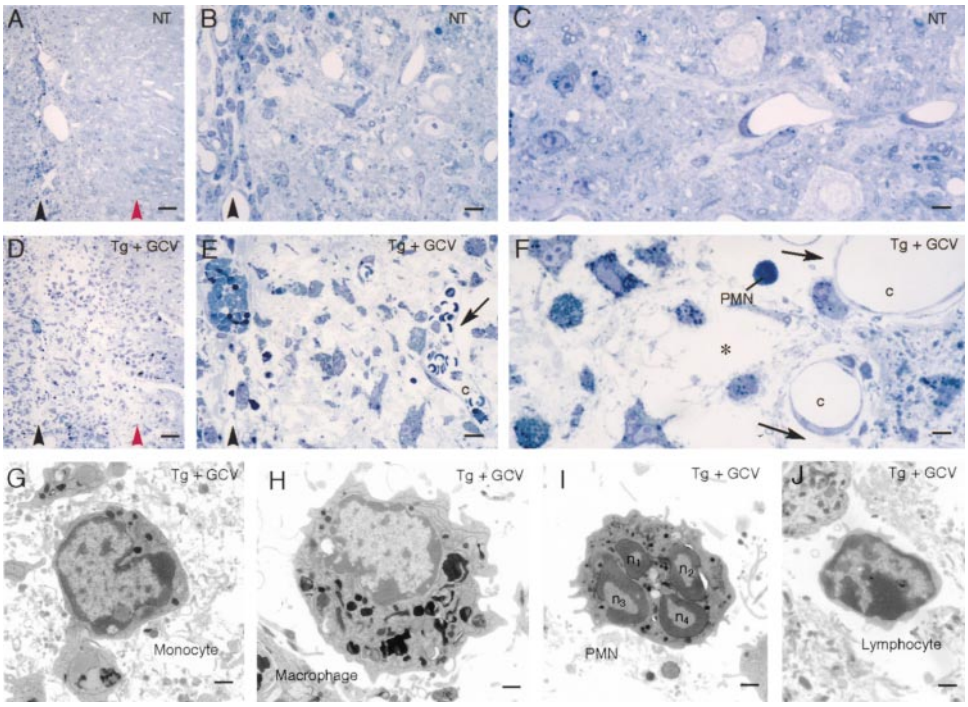

Figure 3. Integrity of Injured Tissue and Leukocyte Morphology

(A–F) Toluidine blue-stained semithin sections of neural parenchyma adjacent to stab injury (arrowheads) in thalamus after 7 day survival. Black and red arrowheads demarcate the zone that either contains proliferating, scar-forming reactive astrocytes in control mice, or from which astrocytes have been ablated in GCV-treated transgenic mice. Scale bars: (A and D), 50 μm; (B and E), 10 μm; (C and F), 4 μm.

(A–C) Nontransgenic control.

(D–F) Transgenic given GCV. Astrocyte ablation is accompanied by interstitial edema (asterisk), infiltration of polymorphic leukocytes, and denuding of capillary (c) walls (arrows). PMN, polymorphonuclear neutrophil.

(G–J) Transgenic given GCV. Electron microscopy of leukocytes in neural parenchyma after astrocyte ablation shows morphologies typical of monocytes (G), macrophages (H), polymorphonuclear neutrophils (I) with lobulated nuclei (n_1–n_4), and lymphocytes (J). Scale bars: (G–J), 1 μm.

stained, globoid, and unbranched CD45-positive cells with the appearance of leukocytes were scattered at low density; and (4) at the ultrastructural level, extravasted leukocytes exhibited morphologies typical of monocytes (Figures 3A–3C and 4C–4E). CD45-positive leukocytes were rare in neural parenchyma at distances greater than 1 mm from the wound margins.

The findings were markedly different in transgenic mice given GCV. In these animals, the center of the stab wound was also defined by a narrow column of inflammatory cells and delimited by a thin layer of fibronectin-positive meningeal cells (Figures 3D, 3E, and 4B). However, within the 400 μm of neural parenchyma immediately adjacent to the wound margin, from which astrocytes had been depleted: (1) at 7 days after stab injury, there was pronounced interstitial edema, numerous blood–borne inflammatory and phagocytic cells, and substantial neuronal degeneration (Figures 3D–3J); (2) blood vessels were markedly dilated and endothelial cells were denuded of cellular contacts at many sites (Figures 3F and 5K–5M); (3) compared with controls, there was a statistically significant ($p < 0.001$) 25-fold greater density of globoid, unbranching CD45-positive leukocytes at 14 days that persisted at 35 days (Figures 4C–4L); and (4) at the ultrastructural level, extravasated leukocytes were common, most of which exhibited morphologies typical of monocytes and activated macrophages, but many polymorphonuclear neutrophils, lymphocytes, and occasional mast cells were present (Figures 3G–3J and 5L). Immediately adjacent to this zone, there were numerous activated, finely branched microglia at 7 or 14 days (Figure 4F). Globoid, unbranching CD45-positive leukocytes were regularly scattered throughout neural parenchyma up to 2 mm or more away from the wound margin. By 21 and 35 days, interstitial edema and microglial activation had resolved and varying degrees of tissue collapse had occurred along wound margins and in hippocampal CA1, but many CD45-positive leukocytes continued to be present in tissue depleted of immunoreactive astrocytes both along and away from the wound margin as in CA1 (Figures 1M, 1N, 2E, and 4H–4J). The pharmacological attenuation of neuronal degeneration in GCV-treated transgenic mice (see below) did not prevent the infiltration of CD45-positive leukocytes into CNS parenchyma at 14 days.

Effects of Astrocyte Ablation and Replacement on BBB Repair

After penetrating injury to the CNS, the BBB is damaged and becomes leaky to endogenous and exogenous blood–borne macromolecules. In rodents, this leakiness is repaired within 10 to 14 days. Because astrocytes have been implicated in establishing and maintaining the BBB, we investigated the effects on BBB repair of

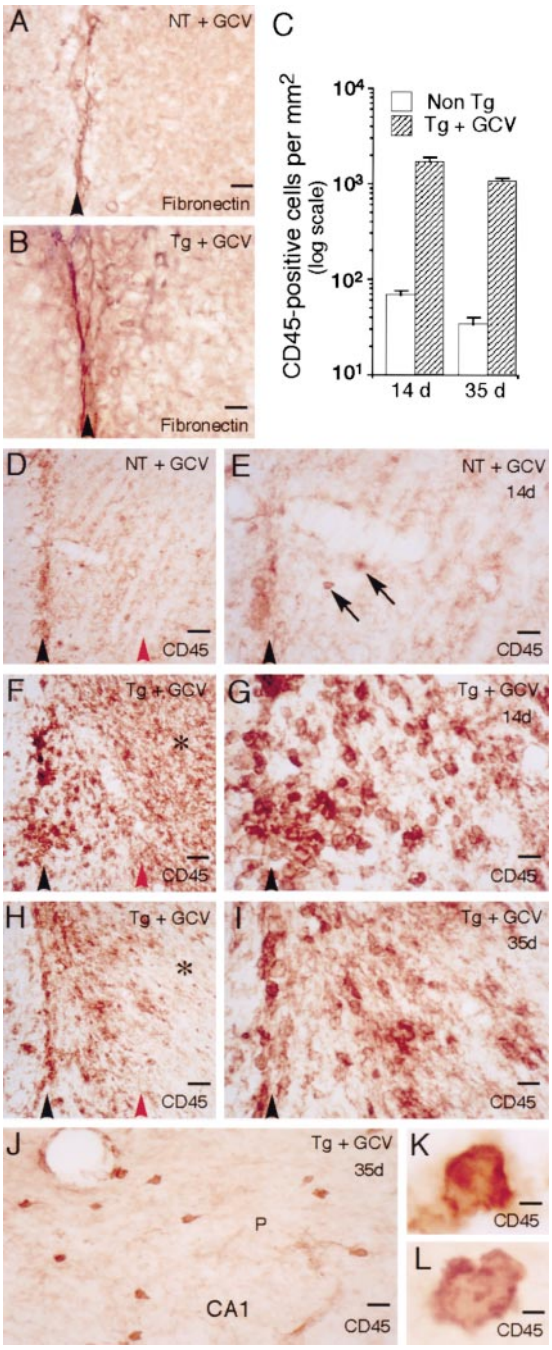

Figure 4. Immunoreactive Meningeal Cells and Leukocytes

(A and B) Immunohistochemistry of fibronectin at the site of stab injury (arrowheads) in the thalamus at 14 days. Staining is not obviously different in nontransgenic (A) and GCV-treated transgenic mice (B). Scale bars, 20 μm.

(C) Mean cell number ± SEM (n = 5 per group) of CD45 immunoreactive cells immediately adjacent to wound margins under different experimental conditions.

(D–L) Immunohistochemistry of CD45 adjacent to stab injury (black arrowhead) in thalamus. Black and red arrowheads demarcate the zone that either contains proliferating, scar-forming reactive astrocytes in control mice, or from which astrocytes have been ablated in GCV-treated transgenic mice. Scale bars: (D, F, and H), 50 μm; (E, G, I, and J), 20 μm; (K and L), 2.5 μm.

(D and E) Nontransgenic control. At 14 days after stab injury, few intensely stained CD45-positive cells with round cell bodies typical of leukocytes (arrows) have entered the neural parenchyma, and there is little evidence of microglial activation.

(F and I) Transgenic given GCV. In the zone of astrocyte ablation, intensely stained, CD45-positive cells with rounded cell bodies typical of leukocytes are densely packed at 14 (F and G) and persist at 35 (H and I) days. Asterisk in (F) and (H) labels tissue adjacent to the zone of astrocyte ablation, which at 14 days contains many (F), and at 35 days few (H), activated microglia with fine, CD45-positive processes.

(J) Transgenic given GCV. In hippocampal CA1, many CD45 positive leukocytes persist at 35 days in areas from which astrocytes have been ablated.

(K and L) Details respectively of (G) and (J).

(1) astrocyte ablation that caused substantial denuding of astrocyte endfeet from blood vessels (Figures 3E, 3F, 5K, and 5L) and (2) astrocyte replacement to such lesions using dispersed cell grafts prepared from astrocyte-enriched tissue cultures of brain tissue from neonatal, nontransgenic mice of line 7.1. To evaluate BBB function, we looked at entry into CNS parenchyma of serum immunoglobulin (IgG) and intravenously injected horseradish peroxidase (HRP), as examples of endogenous and exogenous macromolecules normally excluded from brain parenchyma except at sites that do not exhibit a BBB (Broadwell and Brightman, 1976; Broadwell and Sofroniew, 1993). In uninjured transgenic mice, GCV did not cause detectable disruption of the BBB. At 7 days after stab injury, there was pronounced entry of IgG and HRP into forebrain parenchyma adjacent to the wound in all mice regardless of treatment group (Figure 5A). By 14 days after injury, there was no entry of IgG or HRP at the wound site in control mice, indicating that the BBB had resealed (Figures 5B, 5D, 5G, and 5H). In contrast, after injury in GCV-treated transgenic animals entry of IgG or HRP into parenchyma adjacent to wound margins persisted at all levels along the stab injury at 14, 21, and 35 days (Figures 5C, 5E, 5F, 5I, and 5J). Dispersed cell grafts of astrocytes implanted into the wound area of GCV-treated transgenic mice at 7 or 14 days after injury prevented entry of IgG or HRP into adjacent wound margins in those areas where the grafts were appropriately located and had survived and appeared healthy at 28 or 35 days, indicating that the BBB had resealed (Figures 5N–5R).

Effects of Astrocyte Ablation on Local Neurons

In all three groups of control mice, at all survival times, tissue adjacent to the stab injury in cortex, hippocampus, and thalamus exhibited many healthy neurons surrounded by reactive astrocyte processes, and there was no appreciable loss of neurons (Figures 3A–3C, 6A, 6E, and 6H). In contrast, in GCV-treated transgenic mice, loss of neurons occurred in all brain tissue depleted of astrocytes (Figures 3D–3F, 6B, 6F, 6I, and 6J). Quantitative measurements were performed in hippocampal CA1, where the viability of densely packed pyramidal neurons is easily assessed. In control mice, tissue not containing pyramidal neurons extended for a mean distance of less than 100 μm from the center of the wound (Figure 6D). In GCV-treated transgenic mice, a pronounced loss of pyramidal neurons extended for a mean distance of nearly 1500 μm (Figure 6D). Areas exhibiting

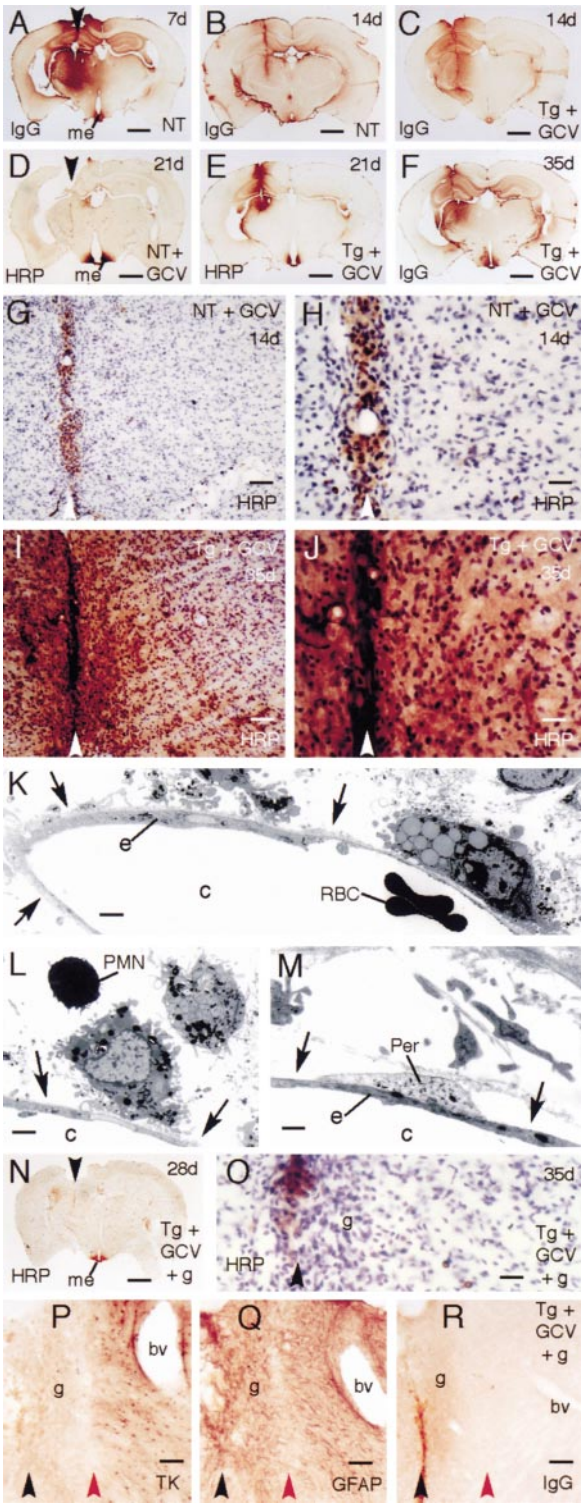

Figure 5. Blood–Brain Barrier

(A–F) Immunohistochemistry of IgG (A–C and F), histochemistry of HRP alone (D and E), and counter-stained with cresyl violet (G–J) after stab injury (arrowheads). Scale bars: (A–F), 1200 μm; (G and I), 120 μm; (H and J), 50 μm.

(A, B, D, G, and H) Nontransgenic. After injury, IgG and HRP enter neural parenchyma at 7 (A), but are excluded at 14 (B, G, and H) and 21 (D) days, except at sites with a normally leaky BBB such as median eminence (me).

(C, E, F, I, and J) Transgenic given GCV. After injury, IgG and HRP continue to enter neural parenchyma at 14 (C, I, and J), 21 (E), and 35 (F) days.

(K–M) Transgenic given GCV. Electron microscopy of tissue near stab injury similar to that in Figure 3F. Capillary (c) endothelial cells (e) are denuded (arrows) of astrocyte endfeet but retain contacts with pericytes (Per) and are surrounded by macrophages, neutrophils (PMN), disorganized neuropil, and cellular debris. RBC, red blood cells. Scale bars: (K), 2 μm; (L), 2.5 μm; (M), 0.8 μm.

(N–R) Transgenics given GCV followed by grafts of nontransgenic cultured astrocytes at 7 (N and P–R) or 14 (O) days. HRP (N and O) and IgG (R) fail to enter neural parenchyma at 28 (N and P–R) or 35 (O) days. Scale bars: (N), 1200 μm; (O), 50 μm; (P–R), 200 μm.

(P–R) Neighboring sections of the same area showing in (P) that TK-positive, transgene-expressing astrocytes are ablated at the stab injury, in (Q) that grafted GFAP-positive, nontransgenic (TK-negative in [P]) astrocytes are resident along the injury, and in (R) that IgG does not enter neural parenchyma along the grafted site. Black and red arrowheads demarcate, respectively, the stab injury and zone from which astrocytes have been ablated. bv, blood vessel; g, graft.

loss of pyramidal neurons corresponded precisely to areas depleted of dividing astrocytes (Figures 2, 6B, and 6F). At the shorter survival time of 7 days, simultaneous visualization of CA1 neurons and GFAP-positive astrocytes revealed that areas depleted of astrocytes furthest away from the stab wound contained many viable CA1 neurons, suggesting that loss of astrocytes preceded loss of neurons (Figure 6K). By 21 or 35 days, there were few surviving neurons, and considerable tissue collapse had occurred (Figure 6B). At 7 days, many CA1 neurons exhibited morphological criteria compatible with excitotoxic cell death, including nuclear condensation with chromatin clumping, vacuolization, membrane disintegration, and dissolution of the cytoplasm (Figures 6I, 6J, and 6L). Because hippocampal neurons are exquisitely sensitive to excitotoxicity, and genetic disruption of glutamate uptake by astrocytes can cause seizures and excitotoxic cell death (Rothstein et al., 1996), we tested the effects of memantine, an antagonist of the N-methyl-D-aspartate (NMDA) glutamate receptor shown previously to attenuate endogenous glutamate-mediated excitotoxicity in transgenic mice (Toggas et al., 1996). In GCV-treated transgenic mice given continuous s.c. memantine, loss of pyramidal neurons extended about 400 μm, representing a significant decrease compared with GCV-treated transgenic mice not given memantine, and a significant increase compared with controls ($p < 0.01$; Figures 6C and 6D).

Effects of Astrocyte Ablation on Local Nerve Fibers

In control mice, tissue that contained scar-forming reactive astrocyte processes in the immediately vicinity of the stab injury exhibited few nerve fibers as revealed with both silver staining and immunohistochemistry for neurofilament M (Figures 7A, 7B, 7E, and 7F). In contrast, in GCV-treated transgenic mice, tissue depleted of astrocytes along the stab injury regularly contained a dense network of randomly oriented fibers (Figures 7C, 7D, 7G and 7H). These fibers were confined to the immediate wound margins depleted of astrocytes and did not extend into adjoining regions that contained surviving reactive astrocytes in neighboring sections. Many fibers

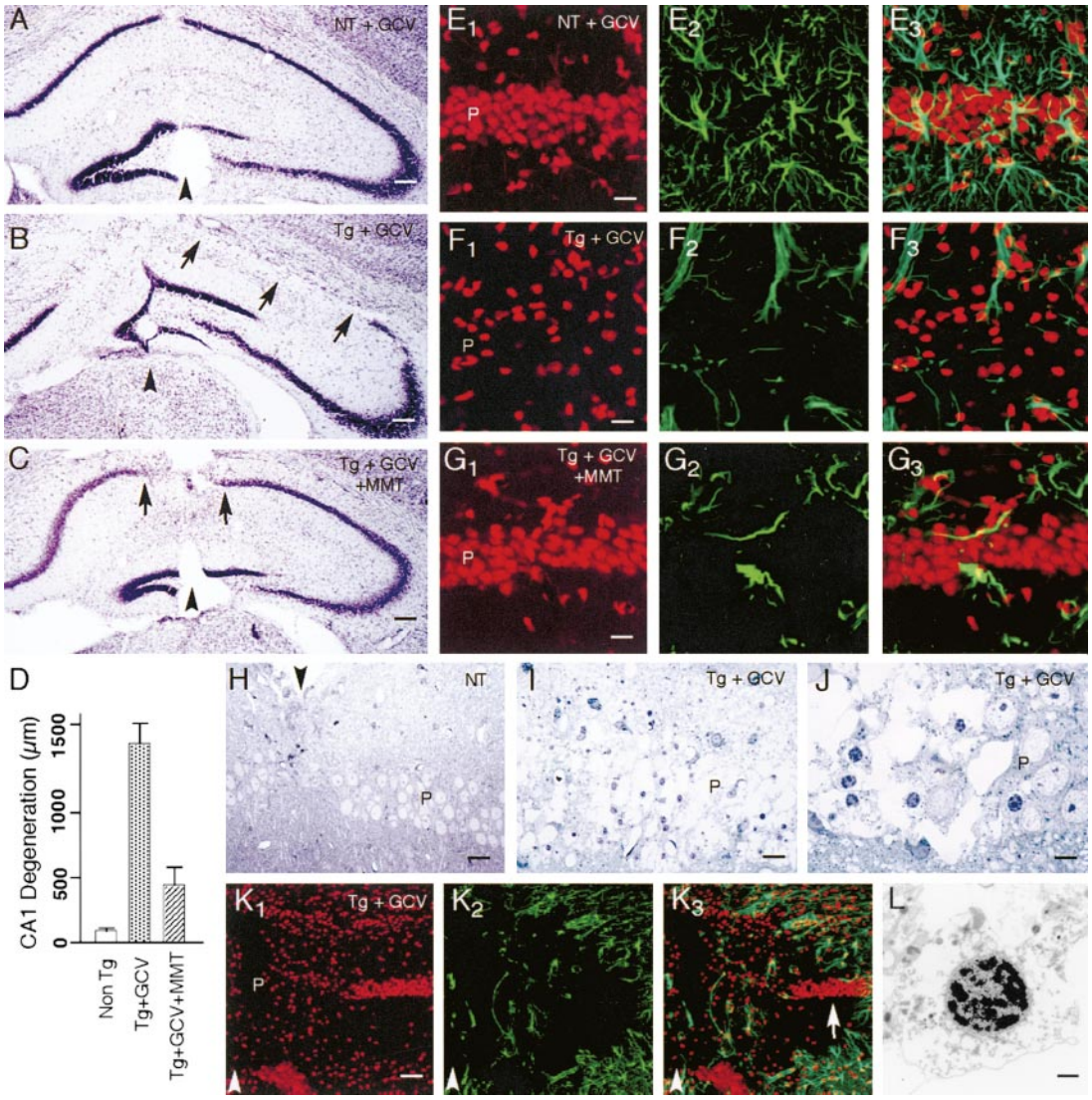

Figure 6. Effects of Astrocyte Ablation on Hippocampal CA1 Pyramidal Neurons

(A–C) Cresyl violet staining of hippocampus after stab injury (arrowheads) under three experimental conditions. In a nontransgenic mouse (A), pyramidal neurons appear healthy. In a GCV-treated transgenic mouse (B), pyramidal neurons have degenerated along the entire length of CA1 (arrows). In a GCV-treated transgenic mouse also given memantine (MMT) (C), pyramidal neurons have degenerated only immediately adjacent to the wound (arrows). Scale bars, 150 μm.

(D) Mean distance ± SEM (n = 8 per group, age-matched females) of the extent of degenerating pyramidal neurons along CA1 under the three experimental conditions shown in (A)–(C).

(E–G) Confocal microscopy of immunofluorescence for GFAP (green) combined with propidium iodide as a nuclear counter-stain (red) shown individually (E_1 and E_2 through G_1 and G_2) and overlaid (E_3, F_3, and G_3) in the CA1 pyramidal layer near stab injury under the same three experimental conditions in (A)–(C). In a nontransgenic mouse (E_1–E_3), many GFAP-positive astrocytes extend processes among pyramidal neurons that appear healthy. In a GCV-treated transgenic mouse (F_1–F_3), astrocytes are ablated and pyramidal neurons have degenerated mice. In a GCV-treated transgenic mouse also given MMT (G_1–G_3), astrocytes are ablated but pyramidal neurons remain viable. Scale bars, 10 μm.

(H–J) Toluidine blue-stained semithin sections of CA1 at 7 days after stab injury. Healthy pyramidal neurons are present immediately adjacent to the wound margin (arrowhead) in a nontransgenic mouse (H), whereas in a GCV-treated transgenic mouse (I and J) pyramidal neurons are degenerating for a considerable distance away from the wound. Scale bars: (H and I), 20 μm; (J), 10 μm.

(K) Confocal microscopy of immunofluorescence for GFAP (green) with propidium iodide (red) in CA1 7 days stab injury (arrowhead) in a GCV-treated transgenic mouse. At this time point, astrocyte ablation extends further along CA1 than does the degeneration of pyramidal neurons (arrow). Scale bar, 80 μm.

(L) Transgenic given GCV. Electron microscopic image of a degenerating pyramidal neuron from the area shown in (J). Scale bar, 1.5 μm.

were finely branched and had a sprouting appearance, and many fibers circled back on each other to run up or down along the wound margin within the area depleted of astrocytes.

Discussion

In this study, we demonstrate the efficacy of a genetic targeting strategy for ablation of scar-forming reactive

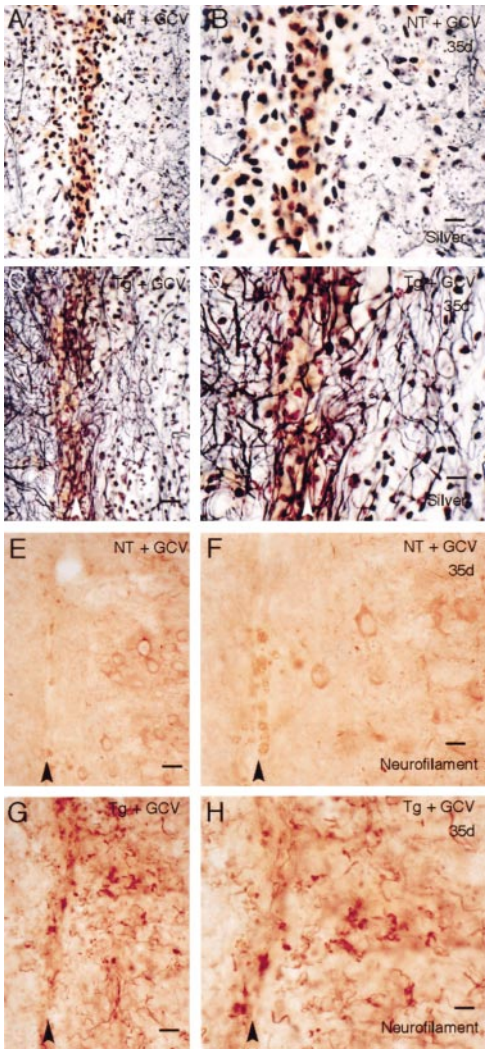

Figure 7. Neurite Outgrowth at Wound Margins

(A–H) Silver staining (A–D) and immunohistochemistry of neurofilament M at the site of stab injury (arrowheads) in the thalamus after 35 days. Scale bars: (A, C, E, and G), 20 μm; (B, D, F, and H), 10 μm.

(A, B, E, and F) Nontransgenic. Few fibers are present in the vicinity of the wound.

(C and D) GCV-treated transgenic. Many fibers extend along the wound margins.

astrocytes after CNS injury. Applying this strategy, we found that loss or dysfunction of reactive astrocytes leads to a prolonged increase in leukocyte infiltration, failure of BBB repair with vasogenic edema, neuronal degeneration, and increased outgrowth of nerve fibers in injured CNS parenchyma.

Subcutaneous GCV Treatment Selectively Ablates Transgene-Expressing Reactive Astrocytes after Forebrain Stab Injury

Our findings show that transgenically targeted HSV-TK combined with 7 days of s.c. GCV allows the selective, site-specific, and temporally regulatable ablation of scar-forming, reactive astrocytes after CNS injury in adult mice. As described previously, 7 days of s.c. GCV in adult transgenic mice did not detectably ablate HSV-TK-expressing, GFAP-positive astroglial cells in major organs, including the uninjured CNS (Bush et al., 1998). GCV does not cross the BBB well (Brewster et al., 1994) but will enter CNS parenchyma at sites of injury where the BBB is compromised. In addition to exposure to GCV, ablation of reactive astrocytes in our mice appeared to require both expression of HSV-TK and induction of cell division after injury, in agreement with studies indicating that after phosphorylation by transgene-derived HSV-TK, GCV-mediated cell death results from formation of toxic intermediates that disrupt DNA replication and preferentially kill dividing cells (Frank et al., 1984; Borrelli et al., 1989). It deserves mention that some nondividing HSV-TK-expressing cells may be killed by an as yet unknown mechanism (Wallace et al., 1991) and that dying astrocytes may be able to injure or kill neighboring astrocytes through specific gap junctions (Budd and Lipton, 1998; Lin et al., 1998). Whether these mechanisms occurred in our mice is not certain but would not have altered the interpretation of our results, which are based on the histologically demonstrated ablation of HSV-TK- and GFAP-positive astrocytes.

Both the specificity and efficacy of our model compare favorably with those of other reported procedures for killing or inactivating astrocytes, such as irradiation, antimitotic agents, and various toxins (Holash et al., 1993; Krum, 1996; Largo et al., 1996). While useful in certain contexts, these procedures are limited by their uncertain specificity for all types of glia or dividing cells in general. Transgenic mice expressing HSV-TK under regulation of a fragment of the human GFAP promoter have been generated by others, who report that single bolus i.p. injections of GCV in the neonatal period disrupt the cytoarchitecture of the developing cerebellum, whereas single GCV injections had no obvious effect on the uninjured adult CNS (Delaney et al., 1996).

Several lines of evidence support the specificity of astrocyte ablation in our model. Under various experimental conditions, nontransgenic mice given GCV were indistinguishable from those not given GCV. In astrocyte-enriched primary cultures of neonatal brains, GCV killed transgene-expressing astrocytes, but neighboring GFAP- and HSV-TK negative fibroblasts and meningeal cells survived and increased in number (Bush et al., 1998). Double-staining immunohistochemical analysis demonstrated at the single cell level that expression of HSV-TK was always restricted to GFAP-positive astrocytes. All transgenic and nontransgenic mice used for comparisons were derived from the same inbred colony and had similar genetic backgrounds, making it unlikely that experimentally induced differences were spurious effects related to genetic background (Choi, 1997). Together, these findings indicate that GCV had no detectable effects on non-transgene-expressing cells, that GCV preferentially killed dividing transgene-expressing astrocytes, and that lethal metabolites of GCV were not released in sufficient quantities by HSV-TK-expressing cells to kill neighboring, non-transgene-expressing cells. Thus, our model is both effective and selective for ablation of scar-forming, reactive astrocytes in the vicinity of CNS injury, providing a novel means of investigating the role of these cells in adult animals.

Astrocytes Regulate Leukocyte Infiltration into CNS Parenchyma

In higher vertebrates, leukocytes gain little entry into normal CNS parenchyma, and the CNS inflammatory response to injury differs from that of other tissues (Dowding and Scholes, 1993; Perry et al., 1993). After injury, neuronal degeneration, or injection of proinflammatory molecules, blood–borne monocytes and lymphocytes gain delayed and limited access to CNS parenchyma, while polymorphonuclear neutrophils and mast cells are largely excluded, suggesting that the CNS microenvironment contains intrinsic, but unknown, antiinflammatory mechanisms (Perry et al., 1993; Hirschberg and Schwartz, 1995; Raivich et al., 1998; Carson and Sutcliffe, 1999). Our findings demonstrate that in the absence of astrocytes, leukocytes gain increased and prolonged entry into CNS parenchyma. Although some of this increase may at short survival times simply represent a heightened response to the presence of dead and dying cells (i.e., transgene-expressing astrocytes killed by GCV or neurons dying secondary to loss of astrocytes), available evidence indicates that this is unlikely to account for the level and duration of the response. Others have reported that after induction of neuronal degeneration using different neurotoxins, the inflammatory response is either composed largely of activated resident microglia or exhibits a modest number of leukocytes that resolve entirely within days or several weeks (Streit and Kreutzberg, 1988; Andersson et al., 1991; Riva-Depaty et al., 1994), indicating that the presence of dead cells on its own is not sufficient to trigger pronounced leukocyte infiltration. In addition, attenuation of neuronal degeneration in our GCV-treated transgenic mice did not prevent infiltration of leukocytes into astrocyte ablated tissue. Thus, it can be argued that the absence of astrocytes contributed directly to both the persisting and polymorphic nature of the increased leukocyte infiltration, particularly after the debris had been cleared at the longer survival times.

It is not yet clear whether the increased leukocyte entry after astrocyte ablation is a consequence of BBB disruption or of other factors. Available evidence suggests that the tight junctional complexes that form the BBB by restricting the passage of macromolecules are not the sole mechanism regulating leukocyte trafficking in the CNS (Carson and Sutcliffe, 1999). Mechanisms by which astrocytes could dynamically modulate the entry of leukocytes into normal or injured CNS parenchyma in addition to, and perhaps independently of, their influence on the tight junctional complexes of the BBB include their ability to produce (1) both pro- and antiinflammatory cytokines (Eddleston and Mucke, 1993; Ransohoff and Tani, 1998) and (2) extracellularly deposited molecules that positively and negatively influence the migration of many cell types and nerve fibers (Blakemore and Crang, 1989; Grumet et al., 1993; Davies et al., 1997). In this context, it is noteworthy that ablation of GFAP-expressing enteric astroglia in our transgenic mice was also associated with pronounced infiltration of small intestine mucosa by polymorphic leukocytes (Bush et al., 1998). Trafficking signals that attract leukocytes to sites of injury and promote extravasation have been identified, but factors that regulate leukocytic migration and localization in specific anatomic compartments are poorly understood (Springer, 1994). Our findings demonstrate that astrocytes play a role in regulating the trafficking of leukocytes into injured CNS parenchyma. Dysfunction of this role represents a novel potential pathogenic mechanism for inflammatory disturbances in the CNS.

Astrocyte Ablation Causes Failure of BBB Repair and Vasogenic Edema

The anatomical correlate of the BBB is thought to reside in tight junctions between endothelial cells of cerebral capillaries, which are of high electrical resistance and present a barrier to charged molecules (Brightman and Reese, 1969; Rubbin and Staddon, 1999). CNS endothelia are not fundamentally different from those in peripheral tissues and are induced to adopt BBB-like properties by unidentified factors in CNS tissue (Stewart and Wiley, 1981). Endothelial cells of cerebral capillaries are enveloped by astrocyte foot processes, and several lines of evidence suggest that astrocytes are important in establishing the BBB: (1) grafts of astrocytes induce BBB-like properties in peripheral endothelia (Janzer and Raff, 1987) and (2) coculture with astrocyte cell lines induces tight junctions and increases the electrical resistance across endothelial and epithelial cell layers in vitro (Hurst and Fritz, 1996; Veronesi, 1996). Astrocyte induction of the BBB has also been challenged by several experimental studies (Holash et al., 1993; Krum, 1996). Our findings demonstrate an essential role for astrocytes in BBB repair and are compatible with a model requiring either direct contact between astrocyte endfeet and blood vessel walls, or the local diffusion of an astrocyte-produced factor(s), for induction of BBB properties in CNS endothelial cells.

Vasogenic brain edema can accompany disruption of the BBB with poor outcome in various clinical settings and has been neuropathologically associated with the pronounced swelling of reactive astrocytes (Klatzo, 1967). It has not been known if the astroglial changes contribute to development of the edema, and if so, whether edema is actively triggered by reactive astrocytes or results from a failure of astrocyte functions. Our findings support the latter possibility and suggest that astrocyte failure could in this manner exacerbate a number of CNS disorders.

Reactive Astrocytes Protect Neurons

Astrocytes, and related astroglia in other neural systems, provide nutritive, neurotrophic, and other supportive functions for neurons (Banker, 1980; Buchanan and Benzer, 1993; Tsacppoulos and Magistretti, 1996; Bush et al., 1998). Our findings demonstrate the essential nature of astrocyte functions for neuronal survival in the injured adult CNS. There are several ways in which ablation of reactive astrocytes could have led rapidly to neuronal death in our mice. Injury is associated with increased levels of extracellular glutamate (Faden et al., 1989), and ablation of genes encoding astrocyte-glutamate transporters is associated with increased seizurigenesis and excitotoxicity (Rothstein et al., 1996). The ability of simultaneously administered NMDA-receptor

antagonist to prevent some but not all neuronal death after ablation of astrocytes suggests that glutamate excitotoxicity contributed to the neurodegeneration we observed. Nevertheless, the partial nature of the protection suggests that in addition to loss of glutamate uptake, other degenerative mechanisms may also have contributed, such as loss of astrocyte-derived growth factors, loss of nutritive and metabolic support, and/or increased numbers and prolonged presence of inflammatory cells. Our findings support and extend other recent evidence that astrocyte loss or dysfunction represents a potentially significant cause of neuronal degeneration (Budd and Lipton, 1998; Lin et al., 1998).

Reactive Astrocytes Restrict the Local Regrowth of Nerve Fibers

The effects of astrocytes on nerve fiber growth varies with their state of differentiation (Hatten et al., 1991). Although CNS astrocytes support neurite outgrowth during development and under certain conditions in adults (Gage et al., 1988; Kawaja and Gage, 1991), evidence accumulated for over a century suggests that after CNS injury, reactive astrocytes are a major obstacle to the regeneration of damaged axons (Ramon y Cajal, 1928; Reier et al., 1983). This suggestion is supported by observations such as: (1) reactive astrocytes at sites of the PNS–CNS transition zone surround and appear to prevent the entry of regenerating peripheral nerves into CNS (Liuzzi and Lasek, 1987); (2) both three-dimensional cultures of mature astrocytes and astrocyte scar tissue maintained in vitro are nonpermissive to axon growth (Fawcett et al., 1989; Rudge and Silver, 1990); and (3) extracellular matrix molecules produced by reactive astrocytes are associated with failure of axon growth (Davies et al., 1997). Our findings extend these observations by demonstrating that genetic targeting can be used to ablate reactive, scar-forming astrocytes within a time frame after injury that could have clinical relevance and provide direct evidence that scar-forming astrocytes limit the growth of nerve fibers after CNS injury in vivo. Our findings support the view that removal of these cells, or neutralization of the molecules responsible for this effect, will be a required component of achieving substantial axon regeneration after injury in the mature mammalian CNS. Failure of axon regeneration and the exclusion of leukocytes from adult CNS parenchyma are both features of higher, as compared with lower, vertebrates (Dowding and Scholes, 1993; Larner et al., 1995). Our combined findings enable us to speculate that inhibition of nerve fiber growth by scar-forming reactive astrocytes may be an indirect biproduct of the evolution of trafficking cues that regulate leukocyte migration in CNS parenchyma, rather than the result of a primary evolutionary pressure against a detrimental consequence of maintaining a CNS environment that is permissive of axon regeneration.

Experimental Procedures

Animals

Transgenic mice used in this study were generated as described (Bush et al., 1998), and all experimental as well as control animals used were obtained by mating heterozygous females with nontransgenic males of line 7.1. Thus, transgenic and nontransgenic control animals were derived from the same inbred line and had similar genetic backgrounds. Genotyping by Southern blot or PCR was confirmed postmortem by immunohistochemical demonstration of HSV-TK. All mice used in experiments were at least 4 months old. Mice were housed in a 12 hr light/dark cycle with controlled temperature and humidity and allowed free access to food and water.

Surgery

Surgery was performed under general anaesthesia using a combination of i.p. injection of 0.3 mg/kg fentanyl and inhalation of halothane in oxygen enriched air. Forebrain stab injuries through cerebral neocortex, subcortical white matter, hippocampus, and thalamus were made with a sterile number 11 scalpel blade held in rodent stereotaxic apparatus (David Kopf, Tujunga, CA). Beginning at the level of Bregma, a 3 to 4 mm longitudinal cut was made parallel to, and 1.5 mm lateral of, the midline, to a depth of 3.5 mm. GCV (Roche, Welwyn Garden, United Kingdom) was administered continuously at a rate of 100 mg/kg/day (Bush et al., 1998) in sterile physiological saline for 7 days via subcutaneously implanted osmotic minipumps (Alzet, Palo Alto, CA). After a loading dose of 20 mg/kg i.p. prior to forebrain stab injury, memantine (Tocris, Bristol, United Kingdom) was administered continuously at a rate of 2 mg/kg/day (Toggas et al., 1996) in sterile saline for 14 days via subcutaneously implanted osmotic minipumps (Alzet). HRP (Type VI, Sigma [Dorset, United Kingdom] 50 mg in 0.5 ml sterile 0.9% saline) was infused intravenously 45 min before transcardial perfusion with mixed aldehydes (Broadwell and Brightman, 1976). Astrocyte-enriched tissue cultures were prepared from brains of neonatal, nontransgenic mice of line 7.1 (Bush et al., 1998); after 28 days of expansion and differentiation in vitro, cell suspensions were prepared and grafted into GCV-treated transgenic mice at 7 or 14 days after forebrain stab injury. Grafts consisted of 1 to 2 μl columns of cells (400,000 cells/μl) placed into two or three sites along the stab injury. Experiments were conducted in accordance with the United Kingdom Animal Scientific Procedures Act, 1986.

BRDU Treatment

Dividing reactive astroglia were labeled on day 3 postinjury by six subcutaneous injections of 10 mg/kg BRDU (Sigma, St. Louis, MO) dissolved in saline plus 0.007 N NaOH every 2 hr. Mice were perfused 11 days later and tissue processed for immunohistochemistry as described below with the following modification: sections were pretreated with 2M HCl for 30 min and then neutralized with three rinses of PBS before addition of primary antibody.

Histology

Under terminal barbiturate anesthesia, mice were perfused transcardially with buffered 4% paraformaldehyde for routine immunohistochemistry, or with either 1.25% or 2.5% glutaraldehyde plus 2% paraformaldehyde for detection of HRP, or for electron microscopy. Brains were removed, postfixed for a further 1–3 hr, and cryoprotected in buffered 25% sucrose overnight. Frozen sections (40 μm) were prepared on a sledge microtome. Immunohistochemistry was performed using biotinylated secondary antibodies (DAKO, Cambridge, United Kingdom), biotin-avidin-peroxidase complex (Vector), and diaminobenzidine (DAB, Sigma) or Vector SG (Vector as developing agents). Primary antibodies were: rabbit anti-HSV-TK (1:25,000; P. Collins), rabbit anti-GFAP (1:25,000; DAKO), rabbit anti-rat IgG at (1:10,000; DAKO), sheep anti-BRDU (1:1000, Maine Biotechnology Services, Portland, ME), rat anti-mouse CD-45 (1:1000; Pharmingen, Oxford, United Kingdom), rabbit anti-fibronectin (1:4000; DAKO), and rabbit anti-neurofilament M (1:10,000; Chemicon, Harrow, United Kingdom). HRP was visualized directly by incubation of sections in DAB (Broadwell and Brightman, 1976). Tomato–lectin (Sigma) binding was visualized with DAB (Acarin et al., 1996). Tissue for electronmicroscopy was treated with osmium tetroxide and embedded in Epon, and semithin sections were prepared at 1 μm and stained with Toluidine blue or ultrathin sections prepared at 50 nm and stained with uranyl acetate and lead citrate.

Morphometry

Cell counts were performed using an unbiased sampling procedure (Gundersen et al., 1988). For counts of immunoreactive astrocytes,

areas of specimens were traced, and 30 × 14,273 μm^2 counting frames per mm^2 were selected at random by a computer-driven microscope stage (Computer Assisted Stereological Toolbox; Olympus, Glostrup, Denmark). For counts of immunoreactive leukocytes, areas extending 400 μm away from, and 800 μm along, the wound margin on one side were traced, and 12 × 10276 μm^2 counting frames per mm^2 were selected by the computer. The number of positive cells per counting frame was determined, and final counts were expressed as number per mm^2. Statistical evaluations were performed by ANOVA with post hoc, independent, pairwise analysis.

Acknowledgments

We thank Dr. P. Collins for HSV-TK antiserum, Dr. J. Skepper for assistance with electron microscopy, S. Jackson, V. Campbell, and Roche for ganciclovir, C. Starr for technical assistance, and A. P. Newman, J. A. Bashford, and I. Bolton for photography. This work was supported by grants from The Wellcome Trust and Action Research to M. V. S. and M. H. J. and an MRC studentship to T. G. B.

Received December 22, 1998; revised May 28, 1999.

References

Acarin, L., Gonzalez, B., Castellano, B., and Castro, A.J. (1996). Microglial response to N-methyl-D-aspartate-mediated excitotoxicity in the immature rat brain. J. Comp. Neurol. *367*, 361–374.

Amat, J.A., Ishiguro, H., Nakamura, K., and Norton, W.T. (1996). Phenotypic diversity and kinetics of proliferating microglia and astrocytes following cortical stab wounds. Glia *16*, 368–382.

Andersson, P.B., Perry, V.H., and Gordon, S. (1991). The kinetics and morphological characteristics of the macrophage-microglial response to kainic acid-induced neuronal degeneration. Neuroscience *42*, 201–214.

Banker, G.A. (1980). Trophic interactions between astroglial cells and hippocampal neurons in culture. Science *209*, 809–810.

Blakemore, W.F., and Crang, A.J. (1989). The relationship between type-1 astrocytes, Schwann cells and oligodendrocytes following transplantation of glial cell cultures into demyelinating lesions in the adult rat spinal cord. J. Neurocytol. *18*, 519–528.

Borrelli, E., Heyman, R.A., Arias, C., Sawchenko, P.E., and Evans, R.M. (1989). Transgenic mice with inducible dwarfism. Nature *339*, 538–541.

Brewster, M.E., Raghavan, K., Pop, E., and Bodor, N. (1994). Enhanced delivery of ganciclovir to the brain through the use of redox targeting. Antimicrob. Agents Chemother. *38*, 817–823.

Brightman, M.W., and Reese, T.S. (1969). Junctions between intimately apposed cell membranes in the vertebrate brain. J. Cell. Biol. *40*, 648–677.

Broadwell, R.D., and Brightman, M.W. (1976). Entry of peroxidase into neurons of the central and peripheral nervous systems from extracerebral and cerebral blood. J. Comp. Neurol. *166*, 257–284.

Broadwell, R.D., and Sofroniew, M.V. (1993). Serum proteins bypass the blood brain barrier for extracellular entry to the CNS. Exp. Neurol. *120*, 246–263.

Buchanan, R.L., and Benzer, S. (1993). Defective glia in the Drosophila brain degeneration mutant drop-dead. Neuron *10*, 839–850.

Budd, S.L., and Lipton, S.A. (1998). Calcium tsunamis: do astrocytes transmit cell death messages via gap junctions during ischemia? Nat. Neurosci. *1*, 431–432.

Bush, T.G., Savidge, T.C., Freeman, T.C., Cox, H.J., Campbell, E.A., Mucke, L., Johnson, M.H., and Sofroniew, M.V. (1998). Fulminant jejuno-ileitis following ablation of enteric glia in adult transgenic mice. Cell *93*, 189–201.

Carson, M.J., and Sutcliffe, J.G. (1999). Balancing function vs. self defense: the CNS as an active regulator of immune responses. J. Neurosci. Res. *55*, 1–8.

Cheng, Y.-C., Huang, E.-S., Lin, J.-C., Mar, E.-C., Pagano, J.S., Dutschman, G.E., and Grill, S.P. (1983). Unique spectrum of activity of 9-[(1,3-dihydroxy-2-propoxy)methyl]-guanine against herpes virus *in vitro* and its mode of action against herpes simplex virus type 1. Proc. Natl. Acad. Sci. USA *80*, 2767–2770.

Choi, D.W. (1997). Background genes: out of sight, but not out of brain. Trends Neurosci. *20*, 499–500.

Davies, S.J.A., Fitch, M.T., Memberg, S.P., Hall, A.K., Raisman, G., and Silver, J. (1997). Regeneration of adult axons in white matter tracts of the central nervous system. Nature *390*, 680–683.

Delaney, C.L., Brenner, M., and Messing, A. (1996). Conditional ablation of cerebellar astrocytes in postnatal transgenic mice. J. Neurosci. *16*, 6908–6918.

Dowding, A.J., and Scholes, J. (1993). Lymphocytes and macrophages outnumber oligodendroglia in normal fish spinal cord. Proc. Natl. Acad. Sci. USA *90*, 10183–10187.

Eddleston, M., and Mucke, L. (1993). Molecular profile of reactive astrocytes—implications for their role in neurological disease. Neuroscience *54*, 15–36.

Faden, A.I., Demediuk, P., Scott Panter, S., and Vink, R. (1989). The role of excitatory amino acids and NMDA receptors in traumatic brain injury. Science *244*, 798–800.

Fawcett, J.W., Housden, E., Smith-Thomas, L., and Meyer, R.L. (1989). The growth of axons in three-dimensional astrocyte cultures. Dev. Biol. *135*, 449–458.

Frank, K.B., Chiou, J.-F., and Cheng, Y.-C. (1984). Interaction of herpes simplex virus-induced DNA polymerase with 9-(1, 3-dihydroxy-2-propoxymethyl) guanine triphosphate. J. Biol. Chem. *259*, 1566–1569.

Gage, F.H., Olejniczak, P., and Armstrong, D.M. (1988). Astrocytes are important for sprouting in the septohippocampal circuit. Exp. Neurol. *102*, 2–13.

Grumet, M., Flaccus, A., and Margolis, R.U. (1993). Functional characterization of chondroitin sulfate proteoglycans of brain: interactions with neurons and neural cell adhesion molecules. J. Cell Biol. *120*, 815–824.

Gundersen, H.J.G., Bendtsen, T.F., Korbo, L., Marcussen, N., Moller, A., Nielsen, K., Nyengaard, J.R., Pakkenberg, B., Sorensen, F.B., Vesterby, A., and West, M.J. (1988). Some new, simple and efficient steriological methods and their use in pathological research and diagnosis. Acta Path. Microbiol. Immunol. Scand. *96*, 379–394.

Hatten, M.E., Liem, R.K.H., Shwlanski, M.L., and Mason, S.A. (1991). Astroglia in CNS injury. Glia *4*, 233–243.

Heyman, R.A., Borrelli, E., Lesley, J., Anderson, D., Richman, D.D., and Baird, S.M. (1989). Thymidine kinase obliteration: creation of transgenic mice with controlled immune deficiency. Proc. Natl. Acad. Sci. USA *86*, 2698–2702.

Hirschberg, D.L., and Schwartz, M. (1995). Macrophage recruitment to acutely injured central nervous system is inhibited by a resident factor: a basis for an immune-brain barrier. J. Neuroimmunol. *61*, 89–96.

Holash, J.A., Noden, D.M., and Stewart, P.A. (1993). Re-evaluating the role of astrocytes in blood–brain barrier induction. Dev. Dyn. *197*, 14–25.

Hurst, R.D., and Fritz, I.B. (1996). Properties of an immortalised vascular endothelial/glioma cell co-culture model of the blood–brain barrier. J. Cell. Physiol. *167*, 81–88.

Janzer, R.C., and Raff, M.C. (1987). Astrocytes induce blood–brain barrier properties in endothelial cells. Nature *325*, 253–256.

Kawaja, M.D., and Gage, F.H. (1991). Reactive astrocytes are substrates for the growth of adult CNS axons in the presence of elevated levels of nerve growth factor. Neuron *7*, 1019–1030.

Kettenmann, H., and Ransom, B.R. (1995). Neuroglia (New York: Oxford University Press).

Klatzo, I. (1967). Neuropathological aspects of brain edema. J. Neuropathol. Exp. Neurol. *26*, 1–13.

Krum, J.M. (1996). Effect of astroglial degeneration on neonatal blood–brain barrier marker expression. Exp. Neurol. *142*, 29–35.

Largo, C., Cuevas, P., Somjen, G.G., Martin del Rio, R., and Herreras, O. (1996). The effect of depressing glial function in rat brain in situ on ion homeostasis, synaptic transmission, and neuron survival. J. Neurosci. *16*, 1219–1229.

Larner, A.J., Johnson, A.R., and Keynes, R.J. (1995). Regeneration in the vertebrate central nervous system: phylogeny, ontogeny, and mechanisms. Biol. Rev. *70*, 597–619.

Lin, J.H.-C., Weigel, H., Cotrina, M.L., Liu, S., Bueno, E., Hansen, A.J., Hansen, T.W., Goldman, S., and Nedergaard, M. (1998). Gap-junction-mediated propagation and amplification of cell injury. Nat. Neurosci. *1*, 494–500.

Liuzzi, F.J., and Lasek, R.J. (1987). Astrocytes block axonal regeneration in mammals by activating the physiological stop pathway. Science *237*, 642–645.

Perry, V.H., Andersson, P.B., and Gordon, S. (1993). Macrophages and inflammation in the central nervous system. Trends Neurosci. *16*, 268–273.

Raivich, G., Jones, L.L., Kloss, C.U.A., Werner, A., Neumann, H., and Kreutzberg, G.W. (1998). Immune surveillance in the injured nervous system: T-lymphocytes invade the axotomized mouse facial motor nucleus and aggregate around sites of neuronal degeneration. J. Neurosci. *18*, 5804–5816.

Ramon y Cajal, S. (1928). Degeneration and Regeneration of the Nervous System. R.M. May, trans. (London: Oxford University Press).

Ransohoff, R.M., and Tani, M. (1998). Do chemokines mediate leukocyte recruitment in post-traumatic CNS inflammation? Trends Neurosci. *21*, 154–159.

Reier, P.J., Stensaas, L.J., and Guth, J. (1983). The astrocytic scar as an impediment to regeneration in the central nervous system. In Spinal Cord Reconstruction, C.C. Kao, R.P. Bunge, and P.J. Reier, eds. (New York: Raven Press), pp. 163–195.

Ridet, J.L., Malhotra, S.K., Privat, A., and Gage, F.H. (1997). Reactive astrocytes: cellular and molecular cues to biological function. Trends Neurosci. *20*, 570–577.

Riva-Depaty, I., Fardeau, C., Mariani, J., Bouchaud, C., and Delhaye, B.N. (1994). Contribution of peripheral macrophages and microglia to the cellular reaction after mechanical or neurotoxin-induced lesions of rat brain. Exp. Neurol. *128*, 77–87.

Rothstein, J.D., Dykes-Hoberg, M., Pardo, C.A., Bristol, L.A., Jin, L., Kunci, R.W., Kanai, Y., Hediger, M.A., Wang, Y., Schielke, J.P., and Welty, D.F. (1996). Knockout of glutamate transporters reveals a major role for astroglial transport in excitotoxicity and clearance of glutamate. Neuron *16*, 675–686.

Rubbin, L.L., and Staddon, J.M. (1999). The cell biology of the blood–brain barrier. Annu. Rev. Neurosci. *22*, 11–28.

Rudge, J.S., and Silver, J. (1990). Inhibition of neurite growth on astroglial scars in vitro. J. Neurosci. *10*, 3594–3603.

Springer, T.A. (1994). Traffic signals for lymphocyte recirculation and leukocyte emigration: the multistep paradigm. Cell *76*, 301–314.

Stewart, P.A., and Wiley, M.J. (1981). Developing nervous tissue induces formation of blood–brain barrier characteristics in individual endothelial cells. Development *84*, 183–192.

Streit, W.J., and Kreutzberg, G.W. (1988). Response of endogenous glial cells to motor neuron degeneration induced by toxic ricin. J. Comp. Neurol. *268*, 248–263.

Toggas, S.M., Masliah, E., and Mucke, L. (1996). Prevention of HIV-1 gp120-induced neuronal damage in the central nervous system of transgenic mice by the NMDA antagonist memantine. Brain Res. *706*, 303–307.

Tsacppoulos, M., and Magistretti, P.J. (1996). Metabolic coupling between glia and neurons. J. Neurosci. *16*, 877–885.

Veronesi, B. (1996). Characterization of the MDCK cell line for screening neurotoxicants. Neurotoxicology *17*, 433–444.

Wallace, H., Ledent, C., Vassart, G., Bishop, J.O., and Al-Shawi, R. (1991). Specific ablation of thyroid follicle cells in adult transgenic mice. Endocrinology *129*, 3217–3226.